Biomaterials Science

RSC Publishing

PAPER

View Article Online
View Journal | View Issue

Cite this: *Biomater. Sci.*, 2013, **1**, 824

Uptake of poly(2-hydroxypropylmethacrylamide)-coated gold nanoparticles in microvascular endothelial cells and transport across the blood–brain barrier†

Christian Freese,*[a] Ronald E. Unger,[a] Robert C. Deller,[b] Matthew I. Gibson,[b,c] Christoph Brochhausen,[a] Harm-Anton Klok[c] and C. James Kirkpatrick[a]

Received 26th February 2013,
Accepted 8th April 2013

DOI: 10.1039/c3bm60050e

www.rsc.org/biomaterialsscience

The facile and modular functionalization of gold nanoparticles makes them versatile tools in nanomedicine, for instance, photothermal therapy, contrast agents or as model nanoparticles to probe drug-delivery mechanisms. Since endothelial cells from various locations in the body exhibit unique phenotypes we quantitatively examined the amount of different sized poly(2-hydroxypropylmethacrylamide)-coated gold nanoparticles internalized into primary human dermal endothelial cells or human brain endothelial cells (hCMEC/D3) by inductively coupled plasma atomic emission spectroscopy (ICP-AES) and visualized the nanoparticles using light and electron microscopy. Poly(2-hydroxypropylmethacrylamide)-coated gold nanoparticles exhibited high uptake into brain endothelial cells and were used to examine transport mechanisms across the blood–brain barrier using a well-established *in vitro* model of the blood–brain barrier. Our results demonstrate that 35 nm-sized gold nanoparticles were internalized best into human brain endothelial cells by a flotillin-dependent endocytotic pathway. The uptake into the cells is not correlated with transport across the blood–brain barrier. We demonstrated that the surface modification of gold nanoparticles impacts the internalization process in different cells. In addition, to evaluating toxicity and uptake potential of nanoparticles into cells, the transport properties across cell barriers are important criteria to classify nanoparticle properties regarding targeted delivery of drugs.

Introduction

Specific tumor detection, targeting of pharmacological substances and visualization of specific factors in the body are some challenges which as yet are not adequately resolved. This is especially true when the brain is the target for anti-tumor drugs, substrates for imaging and medications against aging diseases. Much higher concentrations are necessary, with more harmful side effects due to the strong barrier properties of the brain and the difficulty in overcoming this barrier.[1]

The use of nanoparticles, especially of gold nanoparticles (AuNPs), may be a promising method to solve many problems of contemporary medicine. To profit from the positive properties of AuNPs (chemical stability, narrow size distribution, easy surface functionalization) potential toxic effects need to be determined and toxic compounds excluded. This will ensure a safe biological/medicinal activity after administration of AuNPs in applications such as photothermal tumor therapy,[2,3] biological imaging and drug/gene delivery in patients.[4–7] For these reasons nanoparticle–cell interaction(s) need to be systematically evaluated for every particle type synthesized.[8] Contaminations with stabilizing agents such as sodium citrate (similar to CTAB) should also be prevented to ensure nanoparticle safety.[9] Besides the exclusion of cytotoxicity caused by AuNPs, the uptake potential and methods of uptake of specific nanoparticles in different cell types are of great interest. We recently described the synthesis of a library of different gold-nanoparticles which differ in size, surface modification and surface charge.[10,11] *In vitro* studies demonstrated that primary human dermal microvascular endothelial cells (HDMEC) preferably internalize 35 nm poly(2-hydroxypropylmethacrylamide)-coated gold nanoparticles compared to gold nanoparticles with different neutral-charged polymer shells (*i.e.* PEG) and different sizes.[10] Thus, in addition to manipulating the targeting *via* peptides which lead to an uptake of gold

[a]*REPAIR-lab, Institute of Pathology, University Medical Center of the Johannes Gutenberg University Mainz and European Institute of Excellence on Tissue Engineering and Regenerative Medicine, Langenbeckstrasse 1, D-55101 Mainz, Germany. E-mail: freesec@uni-mainz.de; Tel: +49 (0)6131-173925*
[b]*University of Warwick, Department of Chemistry, Coventry, UK*
[c]*Ecole Polytechnique Fédérale de Lausanne, Lausanne, Switzerland*

†Electronic supplementary information (ESI) available: Detailed information about the cell viability after gold nanoparticle treatment, the microscopic analysis of the internalization process after 4 hours within HDMEC and hCMEC/D3 and the co-localization with flotillin-1-positive vesicles is available online. See DOI: 10.1039/c3bm60050e

nanoparticles into different organs, such as the brain,[12–14] the coating with poly(2-hydroxypropylmethacrylamide) may also act to target gold nanoparticles to cells. Since various endothelial cells in the body which form the inner layer of the vasculature exhibit different phenotypes, the aim of this study was to investigate whether poly(2-hydroxypropylmethacrylamide)-coated AuNPs show variations in internalization with preference for brain endothelial cells compared to microvascular endothelial cells from the skin. Brain endothelial cells generate the blood–brain barrier (BBB) which is a strong, nearly impenetrable and very selective barrier compared to microvascular endothelial cells from other parts of the body.[15] The BBB regulates the entry of substrates into the brain tissue and at the same time protects the brain from xenobiotic and endobiotic substances by means of ATP-binding cassette transporters.[16] Therefore, the goal of this study was to investigate whether the internalization of poly(2-hydroxypropylmethacrylamide)-coated AuNPs into brain endothelium is associated with transport across the blood–brain barrier by using a well-established *in vitro* model system of the BBB. Cytotoxicity tests were performed to exclude negative impact of the AuNPs on cell viability. Differences in the amount of AuNPs internalized were visualized by optical microscopy and then confirmed by transmission electron microscopy (TEM). The amount of AuNPs within the cells was quantified using inductively coupled plasma atomic emission spectroscopy (ICP-AES) and this was compared to the total number applied. In addition, the intracellular location of the gold nanoparticles in dermal and brain endothelial cells was determined by co-localization studies *via* immunofluorescent staining of flotillin-1 and flotillin-2, which have been shown to be markers of late endosomes and lysosomes but belong to a clathrin- and caveolin-independent uptake mechanism.[17] Ultimately, the goal of the *in vitro* studies was to determine whether a unique surface modification is sufficient to target brain endothelial cells specifically and thus increases the uptake. These *in vitro* findings may also help to decrease the variable biodistribution of nanoparticles into other organs and more efficient transport of drugs across the 'barrier' built by endothelial cells into the brain.[18]

Experimental

Synthesis and characterization of gold nanoparticles

The synthesis, the modification procedure and the characterization have already been published.[10,11] In Table 1 the most important characteristics are summarized.

Table 1 Characteristics of poly(2-hydroxypropylmethacrylamide)-coated gold nanoparticles

Nanoparticle	Core diameter[a] (nm)	Final diameter[a] (nm)	UV_{max} [b] (nm)
Hydroxy@Au_{18}	18	23	522
Hydroxy@Au_{35}	35	46	536
Hydroxy@Au_{65}	65	73	555

[a] Diameter of the citrate-stabilized particles determined from dynamic light scattering measured in water. [b] Represents the wavelength with maximum absorbance in the UV-visible spectrum, and is the SPR peak (surface plasmon resonance).

Isolation and cell culture

Human dermal microvascular endothelial cells were isolated from juvenile foreskin as previously described.[10,19] The cells were grown in ECBM supplemented with 15% fetal bovine serum, 2.5 ng mL^{-1} basal fibroblast growth factor and 10 μg mL^{-1} sodium heparin (all Sigma-Aldrich, St. Louis, USA), and penicillin (10 000 U mL^{-1}) and streptomycin (10 000 μg mL^{-1}) on fibronectin-coated culture plates. Herein this medium is termed ECBM culture medium. Cells were used up to passage three.

The human cerebral microvascular endothelial cell line hCMEC/D3 was provided from the group of Pierre-Olivier Couraud (Department of Cell Biology, Institut Cochin, Paris, France) and characterized as described previously.[20] hCMEC/D3 were also cultured on fibronectin-coated culture flasks in ECBM complete culture medium. The cells were sub-cultivated twice a week and used in passages 29–35.

Porcine brain microvascular endothelial cells (PBECs) were isolated from fresh porcine brains as previously described[21] (C. Freese, unpublished work). Isolated cells were directly seeded onto polyester membranes (Corning, NY, USA) and treated with 3 μg mL^{-1} puromycin for three days. To ensure a tight barrier the transendothelial electrical resistance (TEER) was measured beginning from day 6 with an EVOM voltohmmeter (World Precision Instruments, Germany) equipped with an STX-2 chopstick electrode. Cell experiments were started at day 8 after seeding with filters which exhibit a resistance of at least 170 Ω × cm^2. The cells were treated with nanoparticles which were diluted in ECBM culture medium.

All cells were maintained in an atmosphere of 5% CO_2 and 95% humidified conditions at 37 °C.

Cell viability and cytotoxicity assay

Cells were seeded onto fibronectin-coated 96-well plates with ECGM culture medium and cultured to confluence. PBECs were treated at day 8 in culture. Cells were exposed to different concentrations of AuNPs for 24 hours. Cell viability was measured using the CellTiter 96 AQueous non-radioactive assay (Promega, Mannheim, Germany) as recommended by the manufacturer. For the detection of cytotoxicity, caused by the treatment of AuNPs, 50 μL of the cell supernatant was used. The LDH release into the medium was detected by using the CytoTox 96 non-radioactive cytotoxicity assay (Promega, Mannheim, Germany) as recommended by the manufacturer. The release of LDH of untreated cells was used as the control, and the LDH activity of lysed cells was set to 100%.

Treatment with gold nanoparticles, staining and microscopy

Cells were seeded onto fibronectin-coated LabTek chamber slides (Nunc, Roskilde, Denmark) in ECGM culture medium. After 48 hours cells were incubated with a 100 μg mL^{-1}

nanoparticle suspension for 4 h or 24 h. After the incubation period, cells were washed twice with HEPES buffer including 0.2% BSA and then fixed with 3.7% paraformaldehyde at room temperature for 15 minutes. Afterwards cells were washed, permeabilized with 0.2% Triton X-100 and incubated with mouse anti-human CD31 antibody (DakoCytomation, Glostrup, Denmark) and the corresponding secondary antibody (goat anti-mouse Alexa Fluor 488 or 546; Molecular Probes, Carlsbad, USA) at room temperature for 1 hour each. The nuclei were stained with Hoechst 33342 (Sigma-Aldrich, St. Louis, USA). The LabTeks were embedded with GelMount (Biomeda, Natutec, Germany) and analyzed *via* light/fluorescence microscopy (Olympus IX71 with Delta Vision System, Applied Precision, USA). For the co-localization analyses of flotillins and AuNPs the same staining procedure was used as described for CD31 staining. Nevertheless the cells were fixed with methanol/ethanol at room temperature for 15 minutes. Flotillin-1 and flotillin-2 antibodies were purchased from BD Bioscience (Heidelberg, Germany) and were diluted 1 : 100 in 1% bovine serum albumin–PBS.

To analyze the uptake of AuNPs by transmission electron microscopy endothelial cells were seeded onto fibronectin-coated Thermanox coverslips (Nunc, Roskilde, Denmark), treated with AuNPs (10 μg mL^{-1}) as described above and then fixed with cacodylate-buffered glutaraldehyde (Serva, Heidelberg, Germany) (pH 7.2) for 20 minutes. This was followed by a fixation step in 1% (w/v) osmium tetroxide for 2 hours and dehydration in ethanol. Cells were transferred through propylene oxide. Afterwards the samples were embedded in agar-100 resin (PLANO, Germany) and polymerized at 60 °C for 48 hours. Ultrathin sections were cut with an ultramicrotome (Leica Microsystems, Germany), placed onto copper grids and stained with 1% (w/v) uranyl acetate in alcoholic solution and lead citrate. Ultrastructural analysis was performed with a transmission electron microscope, EM 410 (Philips; Eindhoven, Netherlands).

Quantification of internalized AuNPs by ICP-AES

Cells were seeded onto fibronectin-coated 24-well plates. After reaching confluence the medium was replaced by the nanoparticle suspension (10 μg mL^{-1}). After treatment for 4 hours and 24 h the cells were washed with HEPES + 0.2% BSA, detached by trypsin incubation and transferred after the addition of 0.9 mL PBS to microcentrifuge tubes. The cell suspension was stored at −20 °C until analysis. To the cell lysate solution 0.15 mL of aqua regia (3 : 1 hydrochloric acid–nitric acid; both purchased from Fisher Scientific, UK) were added. Following incubation overnight, the samples were then further diluted to 5 mL using MilliQ water to give a total sample volume of 5 mL. These samples were then analyzed for the total gold content by inductively coupled plasma atomic emission spectroscopy (ICP-AES), and the measurement was repeated 3 times.

Statistical analysis

Data were analyzed as indicated with GraphPad Prism version 5.01 for Windows, GraphPad Software, San Diego, California, USA, http://www.graphpad.com.

Results and discussion

Cellular uptake of gold nanoparticles into endothelial cells

Based on the previously published data which demonstrate that the internalization of AuNPs in HDMEC is dependent on the surface modification of the NPs,[10] we determined the uptake of three different-sized poly(2-hydroxypropylmethacrylamide)-coated gold nanoparticles (AuNPs) in brain microvascular endothelial cells (hCMEC/D3) and compared the results with those obtained for dermal microvascular endothelial cells. The AuNPs were prepared by modification of citrate-stabilized gold nanoparticles using thiol-terminated polymers, obtained by RAFT (reversible addition-fragmentation chain transfer) polymerization, as described previously (Table 1).[11]

The different-sized AuNPs on both endothelial cell types exhibited negligible toxic effects as determined by cell viability and cytotoxicity assays (Fig. S1†). A non-toxic concentration of the AuNPs was used to qualitatively visualize the amount of NPs located within the distinct endothelial cells by optical microscopy and confirmed by TEM analysis. The quantification of the amount internalized was determined by ICP-AES. As shown in Fig. S2† the internalized gold nanoparticles could be detected by optical microscopy after 4 hours of treatment. The particles (black dots) were mostly located in the perinuclear region of hCMEC/D3 cells while the AuNPs in HDMEC samples were mostly detected in the periphery or even on the surface of the cells. Since optical microscopy is limited by the resolution, no single particles can be visualized and this prevents image analysis from quantifying the amount of internalized gold nanoparticles. The limitation of the resolution of the optical microscope was also responsible for the inability to visualize 18 nm poly(2-hydroxypropylmethacrylamide) AuNPs (Hydroxy@Au_{18}) within the cells using this method. However, the method is sufficient to determine whether nanoparticles interact with the cells and whether the cell morphology is affected by the treatment with poly(2-hydroxypropylmethacrylamide)-coated gold nanoparticles. The value of optical microscopy is also supported by the results obtained by Braeckmans and colleagues, who demonstrated that the cell morphology changes if the endothelial cells are exposed to high concentrations of gold nanoparticles.[8] This was demonstrated by the rearrangement of the cytoskeleton. In contrast to the results of Braeckmans no changes in the arrangement of the actin filaments were detected in our studies (data not shown). Staining of the membrane can be used to evaluate cytoskeletal and plasma membrane changes after AuNP exposure. However, even after prolonged exposure to AuNPs, no morphological changes of HDMEC or hCMEC/D3 were observed. An increase of internalized AuNPs could be detected in both cell types with time with most gold nanoparticles located in the perinuclear region (Fig. 1). Due to the increased amount of gold within the cells, vesicles loaded with higher amounts of Hydroxy@Au_{18} within cells could also be visualized by optical microscopy after 24 hours exposure. However, the uptake into the cells was not homogeneous which prevents

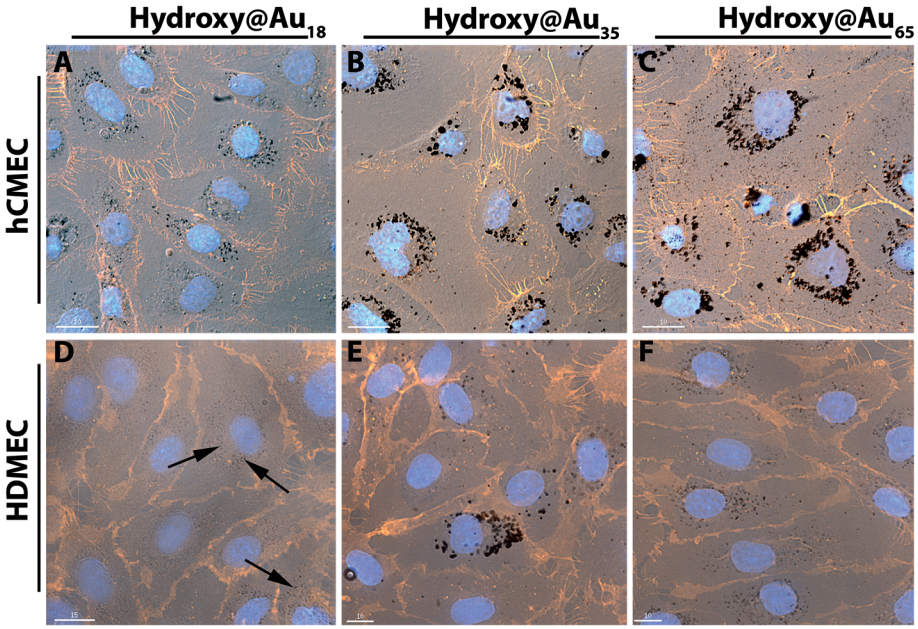

Fig. 1 Detection of poly(2-hydroxypropylmethacrylamide)-coated gold nanoparticles of different sizes in HDMEC and hCMEC/D3 by optical microscopy after 24 hours exposure. hCMEC (A–C) and HDMEC (D–E) were treated with 100 μg mL^{-1} gold nanoparticles at 37 °C for 24 hours. Cell membranes were stained with anti-CD31 antibody and the corresponding secondary antibody (red). Nuclei were stained with Hoechst dye (blue). Agglomerates of gold nanoparticles could be detected as black dots. In (D) agglomerates are quite small, indicated by black arrows. Optical microscopy, Delta Vision (60×). Scale bar: 10 μm (A–C, E–F) or 15 μm (D).

an accurate comparison of internalized AuNPs into the two different cell types by image analysis.

Transmission electron microscopy (TEM) images confirm the internalization and the storage of AuNPs in the perinuclear region within the cells (Fig. S3† and Fig. 2). Using TEM it was possible to detect single gold nanoparticles and to demonstrate that AuNPs were stored in vesicular-like structures in both cell types. None of the nanoparticles were detected in the nucleus. Representative images of the uptake of AuNPs in HDMEC and hCMEC/D3 after a treatment period of 24 hours are presented in Fig. 2. The localization of AuNPs within vesicles (*i.e.*, endosomes and lysosomes) was also described by other groups.[22,23] Endosomal escape has recently been observed for small and ultrasmall AuNPs.[24,25] Liang *et al.* have recently demonstrated that tiopronin-coated AuNPs with sizes of 2 nm–6 nm were found within the nucleus and cytoplasm, while larger AuNPs (15 nm) were only located in the cytoplasm of human breast cancer cells (MCF-7).[26] They speculated that due to the size of the ultrasmall particles (2–6 nm) the AuNPs were able to enter the nuclei *via* the nuclei pores; in contrast the larger particles were prevented from entering the nuclei. Since the smallest poly(2-hydroxypropylmethacrylamide)-coated AuNPs used in this study were larger than 15 nm the distribution within vesicles is in accordance with the results of these groups. Furthermore, the TEM images of the two microvascular endothelial cell types, HDMEC and hCMEC/D3, did not exhibit any differences in the uptake of the different-sized poly(2-hydroxypropylmethacrylamide)-coated gold nanoparticles. However, the amount of AuNPs within the cells increased with time (Fig. S3† and Fig. 2) as shown by optical microscopy and quantified by ICP-AES.

Quantification of internalized gold by ICP-AES

The amounts of internalized poly(2-hydroxypropylmethacrylamide)-coated gold nanoparticles in human dermal microvascular endothelial cells (HDMEC) and human brain microvascular endothelial cells (hCMEC/D3) were quantified by ICP-AES. The quantification was based on an examination of all exposed cells and thus resulted in higher precision compared to high-magnification microscopic image analysis, in which only individual cells were examined. After exposing the cells to gold NPs for 4 and 24 hours, the entire cell population was detached and analyzed after lysis to determine the internalized gold concentration. The percentage uptake of gold NPs applied to cells could be calculated, based on the number of AuNPs within the cells and on the total amount applied to the cells.

Image analysis could not demonstrate any differences in the uptake of poly(2-hydroxypropylmethacrylamide)-coated AuNPs in HDMEC or hCMEC/D3 by the ICP-AES. However, the data presented in Fig. 3A and C demonstrate that the amount of gold nanoparticles within the cells was higher in brain endothelial cells (hCMEC/D3) compared to dermal endothelial cells (HDMEC). This was confirmed by determining the percentage uptake of the gold nanoparticles (Fig. 3B and C). After 4 hours of exposure to nanoparticles, 7.2% (±4.5% SD) of the total amount of the 35 nm-sized gold nanoparticles (Hydroxy@Au_{35}) applied were taken up in HDMEC and 21% (±2.5%) in hCMEC/D3 were internalized. However, with the largest

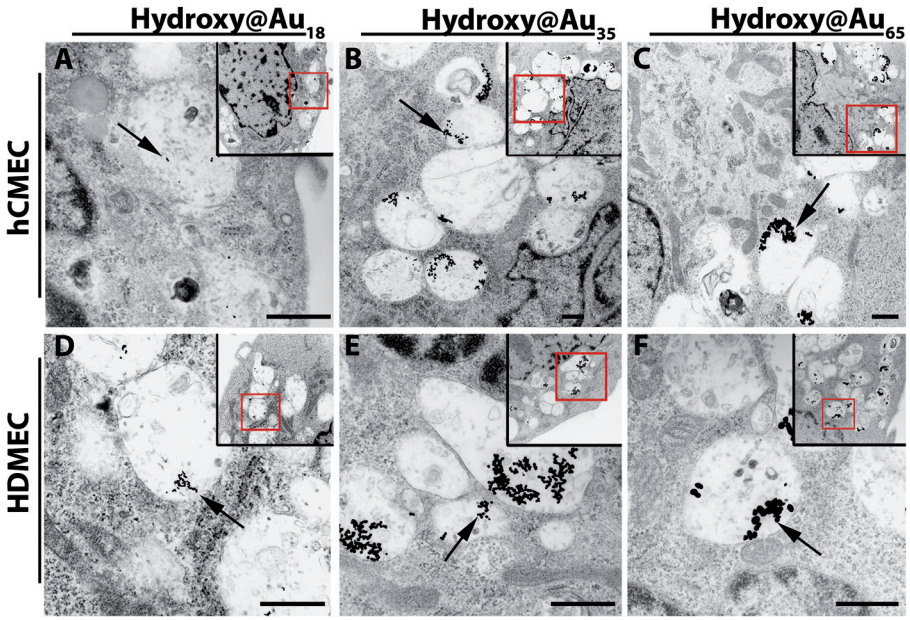

Fig. 2 TEM images of hCMEC/D3 and HDMEC after treatment with different gold nanoparticles for 24 hours. hCMEC/D3 (A–C) and HDMEC (D–F) were treated with 10 μg mL^{-1} gold nanoparticles. Arrows indicate gold nanoparticles within the cells. Images in the corners with the red contours represent the overview of the magnified main image. Images 3500×; small images 2100×. Scale bar: 1 μm.

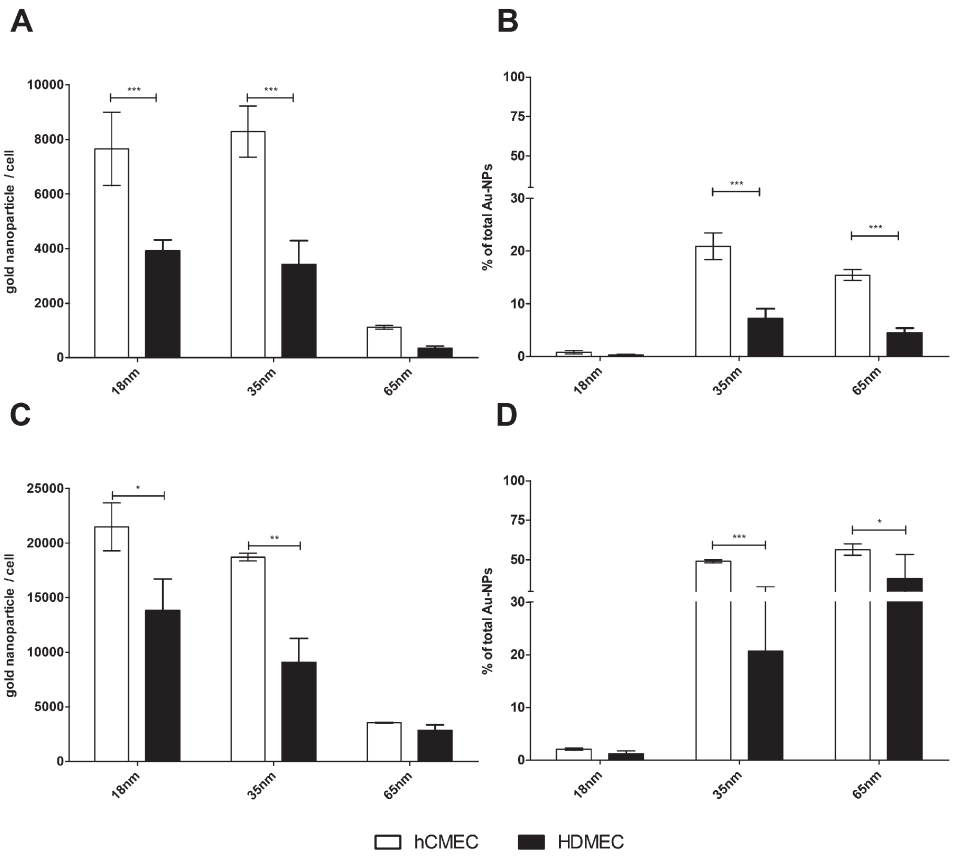

Fig. 3 Quantification of internalized gold nanoparticles in HDMEC and hCMEC/D3 by ICP-AES. hCMEC/D3 and HDMEC were treated with 10 μg mL^{-1} gold nanoparticles for 4 hours (A + B) and 24 hours (C + D). After the incubation cells were extensively washed and collected in a sufficient volume of PBS. After treatment with nitric acid, the total amount of gold in the different wells was measured by ICP-AES (mean ± SD; n = 3–6). Differences in the uptake behavior into HDMEC and hCMEC/D3 were determined by spectroscopy. *$p < 0.05$; **$p < 0.01$; ***$p < 0.001$ (two-way ANOVA with the Bonferroni post test).

particles, Hydroxy@Au_{65}, only 4.5% (±2.0%) and 15.5% (±1.0%) were internalized by HDMEC and hCMEC/D3, respectively. After 24 hours the quantity of gold nanoparticles within the cells increased in both endothelial cell types and a similar ratio in the internalization with respect to NP size and cell type was observed compared to 4 h. Although the number of AuNPs of Hydroxy@Au_{18} was significantly higher in hCMEC/D3 compared to HDMEC even after 4 hours of treatment, the percentage of AuNPs internalized was very low and represents no significant differences in the amount internalized in hCMEC/D3 and HDMEC. This indicates that both measures are of great importance. Although the number of the particles internalized was the highest after 24 hours of NP treatment, most of the applied Hydroxy@Au_{18} were not internalized. For *in vivo* investigations as well as for potential biomedical applications in patients these gold nanoparticles may exhibit a broad biodistribution and may cause unwanted side effects.[18] Therefore a combination of a high number within the cells and a high percentage of uptake of applied gold nanoparticles would be of great importance for medical applications. Based on these assumptions the data could be interpreted as follows. Hydroxy@Au_{35} was internalized best in both endothelial cell types but showed a significantly higher affinity for brain endothelial cells compared to dermal endothelial cells. These results are in accordance with previously published results of various groups which observed the same size effect and determined that a size of approximately 50 nm is preferentially internalized by cells.[27] However, it has never been demonstrated that differences in the uptake in two different microvascular endothelial cell types from different locations in the body exist. We demonstrated that the functionalization of AuNPs by a neutral-charged coating with poly(2-hydroxypropylmethacrylamide) can influence the uptake behaviour in different endothelial cell types and may act as a first targeting to brain endothelium without the conjugation of a specific targeting peptide. In contrast to these observations, a different neutral surface modification such as PEG and glucosamine did not show these cell type-specific effects (Fig. S4†). Thus, one cannot argue that the character of the hCMEC/D3 as a cell line compared to primary HDMEC is crucial for the varying amount of nanoparticles internalized. In addition, in most nanoparticle studies, especially for brain targeting and for transport studies of nanoparticles across the BBB generally, only brain endothelial cell types were analyzed and comparative studies with endothelial cells from other locations were not done. Prades *et al.* have impressively demonstrated that peptide-conjugated AuNPs were internalized by brain endothelial cells and were transported to the brain tissue.[12] However, studies with different endothelial cells from the body were not investigated. It is possible that endothelial cells in other locations of the body actually have a higher affinity to those particles without recognizing the specific targeting peptide that we have shown in this study.

This phenomenon described is characterized as "cell vision" and was first mentioned in the field of nanotoxicology assessment of nanomaterials.[28] The concept of "cell vision" is based on the variable cellular response dependent on the cell type starting at the first contact of the nanomaterial with the cell membrane. "Cell vision" is known to influence the amount of uptake, the fate of NPs within the cell and also the activation of various signalling pathways.[29,30] It is a complementary effect to the effect of the protein corona of nanoparticles which is related to the surface modification and size of the NPs and thus also influences the interaction with cells.[31,32] In terms of nanotoxicology the variable effects on different cell types such as endothelial and epithelial cells have also been demonstrated by our group in recent studies.[9] Herein, we were able to indicate that the effect of "cell vision" of different types of endothelial cells and the formation of a specific protein corona around the 35 nm-sized poly(2-hydroxypropylmethacrylamide) AuNPs can be considered as decisive for the specific uptake in brain endothelial cells.

Although *in vivo* studies are necessary to validate the results observed in our *in vitro* studies, the results of these studies indicate that comparative studies with endothelial cells from various locations are necessary to determine and to define the specific affinity of nanoparticles to the cells in the body.

Evaluation of nanoparticle transport across the blood–brain barrier

We have demonstrated that brain endothelial cells internalize Hydroxy@Au_{35} best. To determine whether a transcellular transport of these particles also takes place an *in vitro* BBB model system was used which is described elsewhere (in the manuscript). Although hCMEC/D3 exhibit typical brain endothelial cell characteristics, primary brain endothelial cells more closely mimic the *in vivo* situation.[20,33] Primary cell cultures generally exhibit higher barrier properties, which are known to prevent paracellular transport of drugs as well as nanoparticles *in vivo*. For this reason, a BBB model was developed using primary porcine brain endothelial cells (PBEC) and shown to exhibit similar characteristics to the human BBB. The model consists of PBEC growing as a monolayer on transwell filters. These cells were exposed to poly(2-hydroxypropylmethacrylamide)-coated gold nanoparticles of different sizes. Quantification of NPs transported across the BBB was determined by ICP-AES. Since any AuNPs transported across the cells were diluted in the volume of media in the lower chamber, 500 μg mL^{-1} AuNPs were applied to the upper chamber to ensure that a measurement of gold by ICP-AES after transport across the barrier model could be determined. The cell viability of PBECs was determined after exposure to various concentrations of AuNPs and no decrease in cell viability was detected as measured by the MTS assay even after treatment with 500 μg mL^{-1} AuNPs (Fig. S5†). In addition, TEM images revealed that the monolayer was not influenced by the treatment of AuNPs at this concentration and that tight junctions between the cells were still present and intact. In addition, the transendothelial electrical resistance (TEER) of the cells was measured throughout exposure to AuNPs. Although the TEER decreased after the application of AuNPs similar results were observed in the untreated control cells and

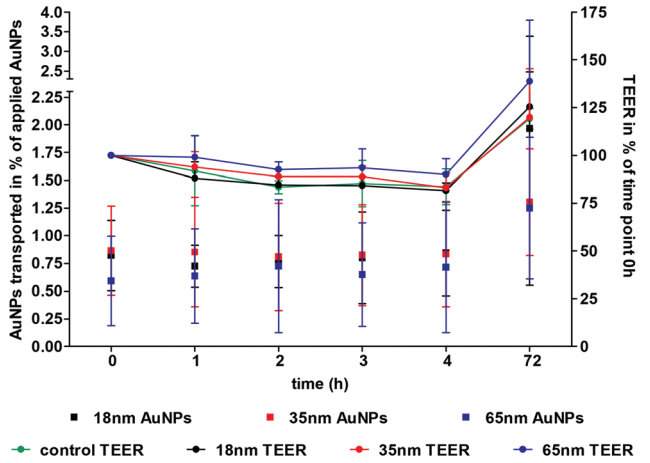

Fig. 4 AuNP concentration measured in the supernatant of the basal chamber after AuNP treatment and transendothelial electrical resistance during the incubation. PBECs on filter membranes of a transwell filter system were stimulated at time point 0 with poly(2-hydroxypropylmethacrylamide)-coated gold nanoparticles. At different time points the AuNP concentration in the lower chamber was determined by ICP-AES and the TEER was measured. The mean of three donors ± SD.

the decrease in TEER is associated with the addition of fresh medium (Fig. 4).[34] After 72 hours of treatment the TEER value was higher than at time point zero, which also excludes a toxic effect of the AuNPs on the brain endothelial cells.

The ICP-AES data in Fig. 4 show that all sizes of poly(2-hydroxypropylmethacrylamide)-coated gold nanoparticles were transported across the cells to a very low degree. After 1 to 4 hours very few gold nanoparticles could be detected. Even after an exposure to nanoparticles for 72 hours, only minimal amounts of AuNPs were detected that had crossed the barrier generated by the PBEC. Prades *et al.* have also demonstrated that a low amount of their AuNPs was transported across an alternate model of BBB.[12] They determined that less than 0.001% citrate-stabilized AuNPs of the total amount initially applied across the co-culture model which consists of bovine microvessel brain endothelial cells and new-born rat astrocytes after 2 hours of treatment were transported. In addition, they demonstrated that AuNPs developed for brain delivery exhibited transport of 0.44% after 2 hours. Thus the transport of maximally 1.1% poly(2-hydroxypropylmethacrylamide)-coated AuNPs (Hydroxy@Au_{18}) examined in our studies across the tight *in vitro* model of the BBB after 72 hours of treatment is in accordance with the results reported by Prades *et al*. The low transport across the BBB is not only restricted to gold nanoparticles. The group of Juillerat-Jeanneret has recently reported that ultrasmall superparamagnetic iron oxide nanoparticles (USPIO-NPs) were internalized by human brain-derived endothelial cells but were not transported across these cells.[35]

Uptake mechanism and intracellular localization of internalized Hydroxy@Au

Due to the low transport properties of different sized Hydroxy@Au across the BBB, we examined the cells to determine whether the particles are internalized by the brain endothelial cells grown on the transwell filters. The TEM images of PBEC indicate that the different-sized poly(2-hydroxypropylmethacrylamide)-coated gold nanoparticles were internalized by the cells and the AuNPs are located in vesicles (Fig. 5). No differences in the uptake of the various sizes of AuNPs were observed. Most of the vesicles in which nanoparticles are stored exhibit multivesicular characteristics. Rago *et al.* have shown that PEG-coated AuNPs were internalized by human squamous carcinoma cells (A431) and were also stored in multivesicular endosomes which are known to be associated with the endosomal degradation pathway.[36,37] In addition to the internalized AuNPs, nanoparticles were found attached to the cell membrane (data not shown). However, in addition uptake events of the nanoparticles were also observed by TEM analysis (Fig. 5D and E).

Based on the TEM analysis and the quantification of results generated by the ICP-AES in analyzing the transport of AuNPs across cells (Fig. 4), it appears that a high uptake of gold nanoparticles does not automatically correlate with a high transcellular transport across the endothelial cell layer.

To determine the specific uptake route and the internal localization of AuNPs that were taken into cells, co-localization studies of NPs with intracellular compartments were undertaken. Cells exposed to AuNPs were stained with fluorescently-labeled antibodies to specific endocytotic organelles and microscope images were analyzed for the location of AuNPs and fluorescence. No co-localization with various endocytotic markers for early endosome antigen-1 (EEA-1), caveolin-1, or clathrin heavy chain, to early endosomes, vesicles which belongs to the clathrin-dependent or caveolin-associated uptake mechanisms, could be detected (data not shown). Based on the TEM images the AuNPs were located within the endosomal/lysosomal vesicles. These vesicles were stained with antibodies to flotillin-1/2 (reggie-2/1). Images showed that the AuNPs (seen as black dots) were surrounded by the flotillin-2-positive membrane staining. Fig. 6 is a representative image of the uptake of the medium-sized poly(2-hydroxypropylmethacrylamide)-coated gold nanoparticles (Hydroxy@$AuNP_{35}$) into hCMEC/D3 stained with antibody to flotillin-2.

The same results were observed for hCMEC/D3 as well as for HDMEC for the flotillin-1 staining (Fig. S6†). These findings confirmed the findings observed by TEM analysis (Fig. 2 and 5) that the gold nanoparticles were encapsulated in vesicle-like structures that were not freely located in the cytoplasm, the mitochondria or the nucleus.

The 'co-localization' of AuNPs and flotillins may reveal that the nanoparticles were internalized *via* a clathrin- and caveolin-independent pathway.[17] In previous studies we have shown that silica nanoparticles of different sizes were also internalized and stored in flotillin-1/2-positive vesicles in human lung epithelial and endothelial cells, NCI H441 and ISO-HAS-1.[19,38,39] In addition we demonstrated that flotillin-1/2 depletion leads to a decrease in uptake and an increase in toxic effects of nanoparticles. This indicates the importance of flotillins in the uptake of nanoparticles. In the present study

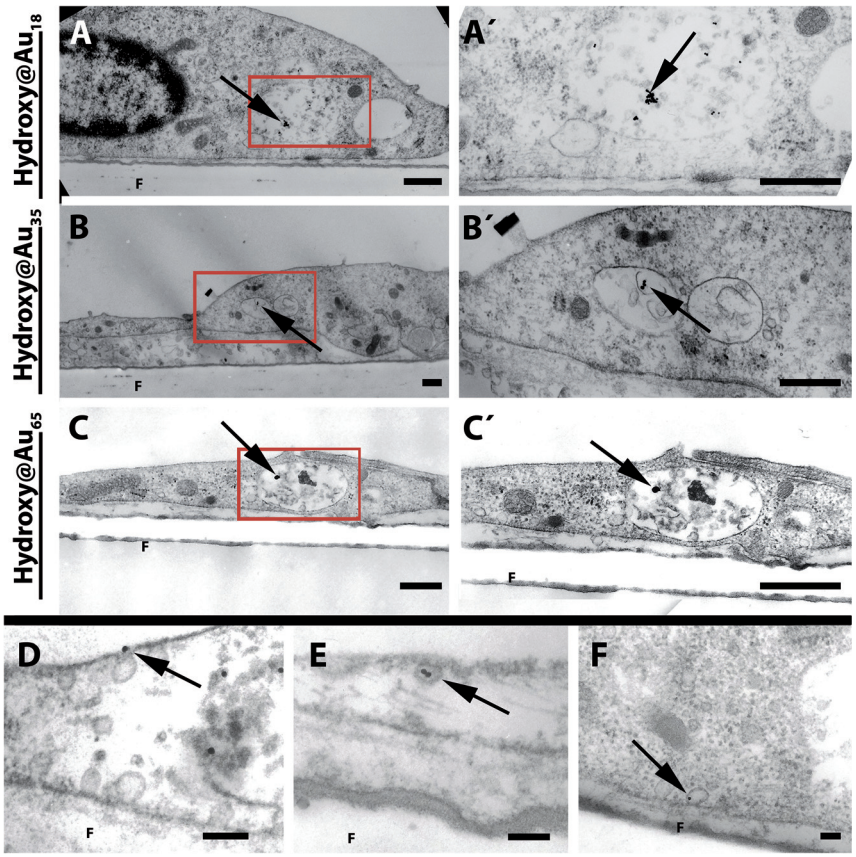

Fig. 5 TEM images of PBEC monolayers treated with poly(2-hydroxypropylmethacrylamide)-coated gold nanoparticles. After the treatment of PBEC grown on filter membranes with different sized AuNPs, cells were fixed with glutaraldehyde and analyzed by transmission electron microscopy. Arrowheads show AuNPs located in vesicles within the cells. Left side (A–C): overview of cells. Right side (A′–C′): magnifications of red boxes of A–C. In D and E uptake events of AuNPs into cells are shown. In E the fusion of an AuNP-loaded intracellular vesicle with the membrane is shown. Scale bar: (A–C) 0.5 μm; (D–F) 0.1 μm. F = filter membrane.

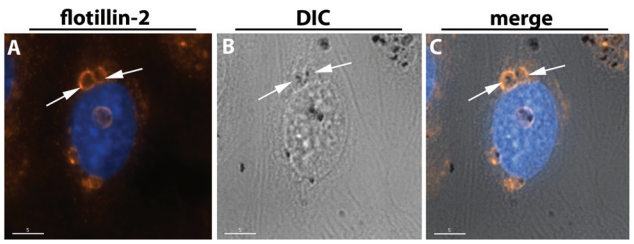

Fig. 6 Co-localization of Hydroxy@AuNP35 with flotillin-2 positive vesicles in hCMEC/D3. hCMEC/D3 were treated with 100 μg mL^{-1} poly(2-hydroxypropylmethacrylamide)-coated gold nanoparticles (Hydroxy@AuNP35) for 24 hours. Cells were stained with anti-flotillin-2 antibody (red) (A). Differential interference contrast (DIC) images are presented in image B, while the merged images are presented in C. Nuclei are stained in blue (Hoechst dye). Delta Vision, 100×. Scale bar 5 μm.

we have shown that AuNPs were also internalized *via* a flotillin-dependent uptake mechanism in human brain and dermal endothelial cells. Flotillins have also been described as a marker for late/lysosomal compartments.[40] In addition, Vercauteren *et al.* described that the trafficking of an internalized nanoparticle containing a medicine *via* Rab5- and flotillin-2-positive vesicles results in a delivery to Rab7 and LAMP1-labeled late endolysosomes, where the nanoparticle was shown to be entrapped for days. This might result in a functional loss of the nanomedicine.[41] Moreover, this could explain the low transport of gold nanoparticles across the blood–brain barrier as described in our studies for poly(2-hydroxypropylmethacrylamide)-coated AuNPs, as well as for AuNPs conjugated to a targeting peptide described by Prades *et al.*[12]

Conclusion

We demonstrated that poly(2-hydroxypropylmethacrylamide)-coated AuNPs were non-toxic to endothelial cells and exhibited a higher affinity for brain endothelial cells compared to dermal endothelial cells and the uptake properties of different coated gold nanoparticles. This provides evidence for a preferential targeting to brain endothelial cells. In addition, we were able to demonstrate that the internalization or uptake of AuNPs is not directly related with the transport of nanoparticles across the endothelial cell barrier. Finally, we have shown for the first time that gold nanoparticles are located within vesicles which are positive for flotillins. This entrapment might explain the low amount of nanoparticles which were transported across the *in vitro* model of the blood–brain barrier.

However, these phenomena now need to be studied in suitable *in vivo* systems.

Acknowledgements

This study has been funded by the FP6 project 'NanoBioPharmaceutics' (NMP4-CT-2006-026723). We wish to thank A. Sartoris, M. Müller, L. Meyer, and K. Molter for their excellent technical assistance. In addition, we thank P.-O. Couraud (Department of Cell Biology, Institut Cochin, Paris, France) for providing us with the immortalized endothelial cell line hCMEC/D3. The equipment used was supported by the Innovative Uses for Advanced Materials in the Modern World (AM2), with support from Advantage West Midlands (AWM), and was partially funded by the European Regional Development Fund (ERDF). Matthew I. Gibson is a Birmingham Science City Interdisciplinary Research Fellow, supported by HEFCE.

References

1 M. I. Alam, S. Beg, A. Samad, S. Baboota, K. Kohli, J. Ali, A. Ahuja and M. Akbar, *Eur. J. Pharm. Sci.*, 2010, **40**, 385–403.
2 W. I. Choi, J.-Y. Kim, C. Kang, C. C. Byeon, Y. H. Kim and G. Tae, *ACS Nano*, 2011, **5**, 1995–2003.
3 D. P. O'Neal, L. R. Hirsch, N. J. Halas, J. D. Payne and J. L. West, *Cancer Lett.*, 2004, **209**, 171–176.
4 V. W. Ng, R. Berti, F. Lesage and A. Kakkar, *J. Mater. Chem. B*, 2013, **1**, 9–25.
5 J. D. Gibson, B. P. Khanal and E. R. Zubarev, *J. Am. Chem. Soc.*, 2007, **129**, 11653–11661.
6 B. Duncan, C. Kim and V. M. Rotello, *J. Controlled Release*, 2010, **148**, 122–127.
7 E. Kim, J. Yang, C. Jihye and S. Haam, *Nanotechnology*, 2009, **20**, 365602.
8 S. J. Soenen, B. Manshian, J. M. Montenegro, F. Amin, B. Meermann, T. Thiron, M. Cornelissen, F. Vanhaecke, S. Doak, W. J. Parak, S. De Smedt and K. Braeckmans, *ACS Nano*, 2012, **6**, 5767–5783.
9 C. Freese, C. Uboldi, M. I. Gibson, R. E. Unger, B. B. Weksler, I. A. Romero, P. O. Couraud and C. J. Kirkpatrick, *Part. Fibre Toxicol.*, 2012, **9**, 23.
10 C. Freese, M. I. Gibson, H.-A. Klok, R. E. Unger and C. J. Kirkpatrick, *Biomacromolecules*, 2012, **13**, 1533–1543.
11 M. I. Gibson, D. Paripovic and H.-A. Klok, *Adv. Mater.*, 2010, **22**, 4721–4725.
12 R. Prades, S. Guerrero, E. Araya, C. Molina, E. Salas, E. Zurita, J. Selva, G. Egea, C. Lopez-Iglesias, M. Teixido, M. J. Kogan and E. Giralt, *Biomaterials*, 2012, **33**, 7194–7205.
13 Y. Cheng, J. D. Meyers, R. S. Agnes, T. L. Doane, M. E. Kenney, A. M. Broome, C. Burda and J. P. Basilion, *Small*, 2011, **7**, 2301–2306.
14 S. Guerrero, E. Araya, J. L. Fiedler, J. I. Arias, C. Adura, F. Albericio, E. Giralt, J. L. Arias, M. S. Fernandez and M. J. Kogan, *Nanomedicine*, 2010, **5**, 897–913.
15 N. J. Abbott, A. A. K. Patabendige, D. E. M. Dolman, S. R. Yusof and D. J. Begley, *Neurobiol. Dis.*, 2010, **37**, 13–25.
16 A. H. Schinkel, *Adv. Drug Delivery Rev.*, 1999, **36**, 179–194.
17 O. O. Glebov, N. A. Bright and B. J. Nichols, *Nat. Cell Biol.*, 2006, **8**, 46–54.
18 W. H. De Jong, W. I. Hagens, P. Krystek, M. C. Burger, A. J. A. M. Sips and R. E. Geertsma, *Biomaterials*, 2008, **29**, 1912–1919.
19 R. E. Unger, V. Krump-Konvalinkova, K. Peters and C. J. Kirkpatrick, *Microvasc. Res.*, 2002, **64**, 384–397.
20 B. B. Weksler, E. A. Subileau, N. Perrière, P. Charneau, K. Holloway, M. Leveque, H. Tricoire-Leignel, A. Nicotra, S. Bourdoulous, P. Turowski, D. K. Male, F. Roux, J. Greenwood, I. A. Romero and P. O. Couraud, *FASEB J.*, 2005, **19**, 1872–1874.
21 R. E. Unger, J. B. Oltrogge, H. Briesen, B. Engelhardt, U. Woelke, W. Schlote, R. Lorenz, H.-J. Bratzke and C. J. Kirkpatrick, *In Vitro Cell. Dev. Biol.: Anim.*, 2002, **38**, 273–281.
22 L. Y. Chou, K. Ming and W. C. Chan, *Chem. Soc. Rev.*, 2011, **40**, 233–245.
23 V. See, P. Free, Y. Cesbron, P. Nativo, U. Shaheen, D. J. Rigden, D. G. Spiller, D. G. Fernig, M. R. White, I. A. Prior, M. Brust, B. Lounis and R. Levy, *ACS Nano*, 2009, **3**, 2461–2468.
24 J. F. Hainfeld, D. N. Slatkin, T. M. Focella and H. M. Smilowitz, *Br. J. Radiol.*, 2006, **79**, 248–253.
25 E. Oh, J. B. Delehanty, K. E. Sapsford, K. Susumu, R. Goswami, J. B. Blanco-Canosa, P. E. Dawson, J. Granek, M. Shoff, Q. Zhang, P. L. Goering, A. Huston and I. L. Medintz, *ACS Nano*, 2011, **5**, 6434–6448.
26 K. Huang, H. Ma, J. Liu, S. Huo, A. Kumar, T. Wei, X. Zhang, S. Jin, Y. Gan, P. C. Wang, S. He, X. Zhang and X.-J. Liang, *ACS Nano*, 2012, **6**, 4483–4493.
27 B. D. Chithrani, A. A. Ghazani and W. C. W. Chan, *Nano Lett.*, 2006, **6**, 662–668.
28 M. Mahmoudi, S. Laurent, M. A. Shokrgozar and M. Hosseinkhani, *ACS Nano*, 2011, **5**, 7263–7276.
29 S. Laurent, C. Burtea, C. Thirifays, U. O. Hafeli and M. Mahmoudi, *PLoS One*, 2012, **7**, e29997.
30 J. Rauch, W. Kolch and M. Mahmoudi, *Sci. Rep.*, 2012, **2**, 868.
31 M. Mahmoudi, S. N. Saeedi-Eslami, M. A. Shokrgozar, K. Azadmanesh, M. Hassanlou, H. R. Kalhor, C. Burtea, B. Rothen-Rutishauser, S. Laurent, S. Sheibani and H. Vali, *Nanoscale*, 2012, **4**, 5461–5468.
32 M. Lundqvist, J. Stigler, G. Elia, I. Lynch, T. Cedervall and K. A. Dawson, *Proc. Natl. Acad. Sci. U. S. A.*, 2008, **105**, 14265–14270.
33 A. Kunzmann, B. Andersson, T. Thurnherr, H. Krug, A. Scheynius and B. Fadeel, *Biochim. Biophys. Acta*, 2011, **1810**, 361–373.
34 R. Rempe, S. Cramer, S. Huwel and H. J. Galla, *Biochem. Biophys. Res. Commun.*, 2011, **406**, 64–69.

35 B. H. Kenzaoui, C. C. Bernasconi, H. Hofmann and L. Juillerat-Jeanneret, *Nanomedicine*, 2012, **7**, 39–53.
36 G. Rago, B. Bauer, F. Svedberg, L. Gunnarsson, M. B. Ericson, M. Bonn and A. Enejder, *J. Phys. Chem. B*, 2011, **115**, 5008–5016.
37 B. Alberts, D. Bray, J. Lewis, M. Raff, K. Roberts and J. D. Watson, *The Cell*, Garland Publishing Inc., New York, 1994.
38 J. Kasper, M. I. Hermanns, C. Bantz, O. Koshkina, T. Lang, M. Maskos, C. Pohl, R. E. Unger and C. J. Kirkpatrick, *Arch. Toxicol.*, 2012, DOI: 10.1007/s00204-012-0876-5.
39 J. Kasper, M. I. Hermanns, C. Bantz, S. Utech, O. Koshkina, M. Maskos, C. Brochhausen, C. Pohl, S. Fuchs, R. E. Unger and C. James Kirkpatrick, *Eur. J. Pharm. Biopharm.*, 2012, DOI: 10.1016/j.ejpb.2012.10.011.
40 J. F. Dermine, S. Duclos, J. Garin, F. St-Louis, S. Rea, R. G. Parton and M. Desjardins, *J. Biol. Chem.*, 2001, **276**, 18507–18512.
41 D. Vercauteren, H. Deschout, K. Remaut, J. F. Engbersen, A. T. Jones, J. Demeester, S. C. De Smedt and K. Braeckmans, *ACS Nano*, 2011, **5**, 7874–7884.